Band gap narrowing and radiative efficiency of silicon doped GaN

H. P. D. Schenk,[1,a)] S. I. Borenstain,[1] A. Berezin,[1] A. Schön,[1] E. Cheifetz,[1] S. Khatsevich,[2] and D. H. Rich[2]

[1]*El-Mul Technologies Ltd., P.O. Box 571 Soreq, Yavne 81104, Israel*
[2]*Department of Physics, Ilse Katz Center for Meso and Nanoscale Science and Technology, Ben-Gurion University of the Negev, P.O. Box 653, Beer-Sheva 84105, Israel*

Radiative efficiency, band gap narrowing, and band filling are studied in Si-doped GaN films as a function of carrier concentration (n), using room and low temperature cathodoluminescence (CL). Using the Kane model, a band gap narrowing ΔE_g of $-(3.6 \pm 0.6) \times 10^{-8}$ and $-(2.6 \pm 0.6) \times 10^{-8} \, n^{1/3}$ eV $n^{1/3}$ is obtained for epitaxially strained and relaxed material, respectively. Band-edge CL time response and absolute external photon yield are measured. The internal radiation efficiency is deduced. Its monotonic increase as n increases is explained by the increase in the spontaneous radiative rate with a radiative free carrier band-to-band recombination coefficient $B = (1.2 \pm 0.3) \times 10^{-11}$ cm^3 s^{-1}. © *2008 American Institute of Physics*. [DOI: 10.1063/1.2919775]

I. INTRODUCTION

Precise knowledge of the parameters governing the GaN luminescence characteristics is imperative for the design of new or improved optoelectronic devices.[1] Band gap renormalization[1–3] (BGR) plays an important role in the design of bipolar devices with heavily doped regions. In spite of the impressive progress made in epitaxial growth and fabrication of GaN based devices,[4] there is a controversy over the value of the band gap narrowing (BGN). Luminescence experiments do not directly reveal it because of being obscured by band-filling induced blueshift, known as the Burstein–Moss shift.[5] According to standard calculation,[1] band filling becomes important above a free electron concentration of 1.75×10^{18} cm^{-3}, when the Fermi level moves into the conduction band. Consequently, evaluation of the BGN based on the room temperature (RT) photoluminescence (PL) *peak* energy alone[6] is underestimated because band filling is ignored. On the other hand, the BGN is overestimated if its determination is based on the low energy luminescence tail.[7] The latter becomes increasingly important with n for it is the result of radiative recombination from potential fluctuation states caused by random distribution of the dopants.[1,8] In the present work, we therefore use the band-edge (BE) luminescence peak and the line shape to reveal the BGN. The Kane model,[1,9] which inherently takes into account both band-filling and donor-induced potential fluctuations, is applied to fit these spectra. We provide a comprehensive framework that includes the investigation of the BGN into a study of the carrier recombination rates in order to quantify the radiative efficiency. A value for the radiative recombination coefficient B is obtained.

II. EXPERIMENT

GaN films were grown by metal-organic chemical vapor deposition on 2 in. *c*-plane sapphire substrates using standard growth conditions.[4,10] Nonintentionally doped (NID) GaN layers, characterized by n in the low to the mid 10^{17} cm^{-3}, are first grown as buffer. Intentionally doped layers (1.5–2.3 μm thick) were grown atop. Total thickness of the epitaxial structures thus varies between 2.5 and 4 μm. Concentrations ranging from 10^{18} to 10^{19} cm^{-3} are obtained by Si doping. In one sample, n in the low 10^{17} cm^{-3} is obtained by compensation with magnesium.

RT cathodoluminescence (CL) spectra were acquired in a vacuum chamber using an 8 keV electron beam with a spot size of 0.5 mm. The light emitted from the film side was collected by a monochromator using slit widths of 500–2000 μm. High e-beam current (42 nA) has been chosen in order to saturate the yellow luminescence.[11] Complementary temperature dependent CL spectra were acquired using a modified JEOL JSM-5910 scanning electron microscope (SEM) with cooled sample stage.[12] Spectra were analyzed using 250 μm entrance slit opening.

Equally, the absolute external UV photon yields were evaluated. The e-beam (8 keV, 5 nA) was accelerated toward the film side of the sample. The emitted light was detected by a single photomultiplier tube (PMT) with the UV pass filter mounted in front of its entrance and compared with the CL intensity collected from a phosphor with a calibrated two-facet UV photon yield of 24 photons/8 kV electron.

RT CL time decay measurements were performed using a vacuum chamber. A double-multichannel plate (MCP) was placed between the e-beam and the sample. Each electron coming from the e-gun triggered a cascade of some 10^6 at 300 fs electrons within the double MCP, which then excited the sample. Two fast PMTs were connected to a photon counting system. PMT-1 registered the photon avalanche generated by the electron-excited radiative decay in the film that triggered the photon counting system. The latter provided a time histogram of single photons received by the

---

a)Author to whom correspondence should be addressed. Present address: CRHEA-CNRS, Rue Bernard Grégory, Sophia Antipolis, 06560 Valbonne, France. Electronic mail: ds@crhea.cnrs.fr. Tel.: 0033 493 95 78 28. FAX: 0033 493 95 83 61.
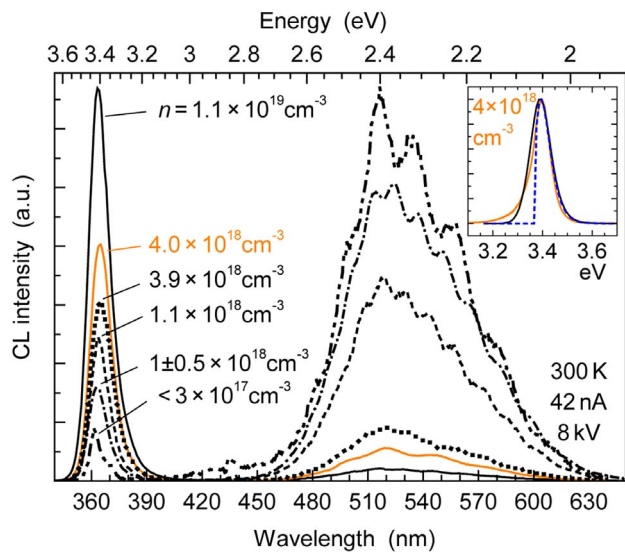
FIG. 1. (Color online) RT CL spectra of NID and Si-doped GaN for various free electron concentrations n. Detail: Typical BE luminescence (orange), and fits assuming the DOS being proportional to $\sqrt{E_e - E_g}$ (broken line), or including a band tail according to the Kane model (black line). Smaller monochromator slit width was used for recording the BE luminescence in detail.

PMT-2 as a function of the time difference with the pulse arrival detected by the PMT-1. UV CL time response was measured using the UV pass filter.

III. RESULTS AND DISCUSSION

CL spectra for various GaN samples with different free electron concentrations were acquired with e-beam energies ranging from 2–24 keV . While the BE luminescence intensity proportionally increases with the e-beam energy above 6 keV, it rapidly reduces below. It is likely that surface recombination is responsible for these high losses since 99% of the incoming electron energy is dissipated in the solid within a depth of penetration less than 0.2 μm. On the other hand, above 8 keV effects of self-absorption become visible in the evolution of the BE intensity as well of its peak energy (redshift). 8 keV have therefore been chosen as standard beam energy. The penetration depth of then <0.3 μm guarantees that all recombination processes occur within the investigated layers.

Typical 8 keV CL spectra of GaN samples with different free electron concentrations are shown in Fig. 1. While the CL spectrum of the NID GaN, $n < 3 \times 10^{17}$ cm^{-3} is dominated by emission from the yellow band (YB), the spectrum of the heavily Si-doped sample $n = 1.1 \times 10^{19}$ cm^{-3} is dominated by BE emission with a maximum intensity near 3.41 eV. Radiative recombination in highly silicon-doped GaN is thus dominated by BE transitions.

In Fig. 2(a), the BE peak energy is plotted as a function of n. It exhibits a redshift from 3.435 to 3.395 eV as the electron concentration increases from low 10^{17} cm^{-3} to the mid 10^{18} cm^{-3}, and a subsequent blueshift with further increase in n. The redshift is due to BGR while the blueshift is the Burstein–Moss band filling effect.[5] As outlined above, the evolution of the luminescence peak alone cannot repre-
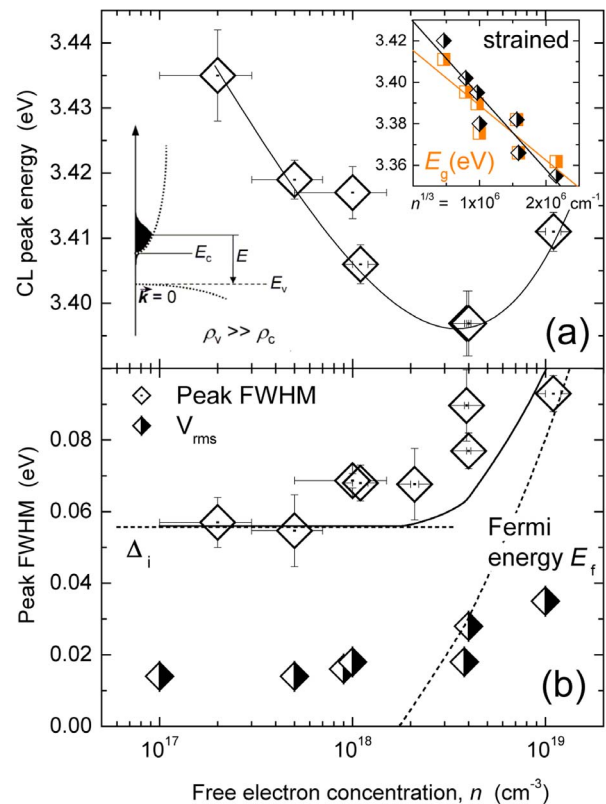

FIG. 2. (Color online) (a) CL peak energy as a function of the free electron concentration n in the sample. The black line is a guide to the eye. Inset: Band gap energy (E_g) vs cubic root of n (diamonds). Squares (orange) include strain correction. (b) The FWHM of the BE luminescence and the band tail parameter (V_{rms}) are plotted as a function of n. V_{rms} is the root-mean-square of the band gap potential fluctuation, extracted from fits to the spectra. Black line: Root mean squares sum of the intrinsic broadening (Δ_i) and the Fermi energy (E_f). Open symbols represent primary experimental data; half filled symbols represent values that are extracted from fits of the BE CL using Eq. (3).

sent the BGR. In order to expose the band gap energy, we use a fit[9] to our spectra based on the calculated radiative recombination described in the following. The generation-recombination rate-equation under steady-state condition of electron-hole pairs is given by[13]

$$\frac{P_r}{3n_{\mathrm{excited}}E_g} = R_{\mathrm{sp}} + \frac{1}{\tau_{\mathrm{NR}}} = \frac{1}{\tau_{\mathrm{eff}}}, \qquad (1)$$

where P_r is the power of the exciting e-beam in watts per unit volume, n_{excited} is the density of excited electron-hole pairs, E_g is the BE energy, and τ_{eff} is the effective (measured) radiative time. The nonradiative decay time τ_{NR} includes all the relaxation processes not related to the BE emission namely transitions to deep level radiative centers (e.g., YB), or to nonradiative defect centers such as dislocations. Contribution from bound excitons is negligible at RT.[14]

The BE total spontaneous emission rate R_{sp} is given by $R_{\mathrm{sp}} = \int R_{\mathrm{sp}}(E)dE$, where E is the photon energy near the BE. Basic material parameters can be extracted by fitting the experimental CL spectra to the theoretical description of $R_{\mathrm{sp}}(E)$,[1]

$$R_{sp}(E) = B \int_{-\infty}^{\infty} \rho_c(E_e)\rho_v(E_h)f_c(E_e)[1 - f_v(E_h)]dE_e, \quad (2)$$

where the hole energy E_h is constrained by the photon energy E and the electron energy E_e by $E = E_e - E_h$, f_c and f_v are the occupation probabilities given by the Fermi–Dirac distribution $f_c(E_e) = [1 + \exp(E_e - E_f)/kT]^{-1}$ and similarly for the valence band, and k is the Boltzmann constant. The factor B is derived from basic quantum mechanical considerations,[15] assuming here an energy independent matrix element. The density of states (DOS) in the conduction (valence) band ρ_c (ρ_v) is proportional to $m_e^{*3/2}$ ($m_h^{*3/2}$), where m_e^* (m_h^*) is the electron (hole) effective mass. Since the hole mass, anywhere between 0.8 and 2.2 (Ref. [16]) is much larger than the electron mass, $m_e^* = 0.2$, making $\rho_v \gg \rho_c$ per dE_e (dE_h). The excited holes are present only in a small energy region at the valence-band top. Consequently, for n-type material, Eq. (2) can be simplified as

$$R_{sp}(E) = B\rho_c(E_e)f_c(E_e). \quad (3)$$

Thus, an obtained spectrum $I(E) \propto R_{sp}(E)$ directly reflects the electron population in the conduction band states as a function of energy. A doping level dependent joint DOS, ρ_c, was formulated by Kane.[1,9] Under sufficiently high doping level, potential fluctuations introduced by ionized impurity states create exponential DOS below the conduction band that merge with the conduction-band free-electrons DOS,

$$\rho_c(E_e) \propto \int_{-\infty}^{(E_e - E_g)/\eta_c} \left(\frac{E_e - E_g}{\eta_c} - z \right)^{1/2} \exp(-z^2)dz, \quad (4)$$

where $\eta_c = \sqrt{2}V_{rms}$ and V_{rms} is the root-mean-square of the potential fluctuations due to ionized impurities.[1] At a finite temperature given the carrier concentration n, the Fermi energy E_f is found by solving the following implicit integral equation:

$$n = \frac{1}{2\pi^2} \left(\frac{2m_e^*}{\hbar^2} \right)^{3/2} \int_0^\infty \frac{\rho_c}{1 + \exp[(E - E_f)]/kT}dE, \quad (5)$$

where $\hbar$ is the Planck constant. Note that as a result of Eq. (5), the Fermi level moves into the conduction band above the free electron concentration of 1.75×10^{18} cm^{-3}. See Fig. 2(b).

An example fit to a CL spectrum, using both the ideal semiconductor model, where the DOS is given by $\rho_c \propto \sqrt{E_e - E_g}$, and the Kane model is shown in the inset of Fig. 1. The ideal semiconductor model cannot account for the tail of the luminescence below the band gap. Although the Kane model accounts for the donor induced potential fluctuations, it cannot fully account for the low energy tail neither. This may be due to the YB. These are defect-induced states occupying a broad region of the gap, which can eventually overlap with near BE (and notably band tail) states. The high-energy side of the peak is determined by the electron thermal distribution described by the Fermi–Dirac distribution. Using the Kane model, we can nevertheless extract the band gap E_g, the Fermi energy E_f, η_c, and the electron concentration (n), which is found to agree with the sample specifications, as determined by RT Hall-effect measurements.
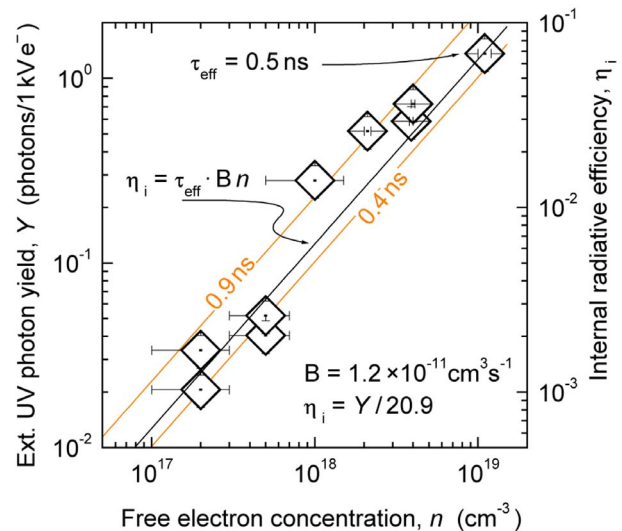

FIG. 3. (Color online) External and internal BE CL efficiency of compensated, NID, and Si-doped GaN for various free electron concentrations. Values for the external BE CL efficiency are normalized according to the number of photons obtained per 1 keV of injected electron energy. τ_{eff} is the effective (measured) radiative time.

The inset of Fig. 2(a) shows the extracted values of E_g plotted as a function of the cubic root of n yielded from the fit, and a least-squares fit to it, $E_g = 3.429 \pm 0.008$ eV $-(3.58 \pm 0.6) \times 10^{-8} n^{1/3}$ eV cm. Note that the model by Jain *et al.*[2] does not yield a reliable improvement to the fit.

By correcting the band gap for the strain-related energy shift $\Delta E_g/\varepsilon_1 = -(9 \pm 0.5)$ eV,[17] caused by the doping-induced lattice deformation $\varepsilon_1 = (a - a_0)/a_0$,[18] we obtain the band gap energy for relaxed material. The respective least-squares fit is $E_g = 3.415 \pm 0.008$ eV $-(2.56 \pm 0.6) \times 10^{-8} n^{1/3}$ eV cm. Our BGN of $\sim 3.6 \times 10^{-8} n^{1/3}$ eV cm for strained and of $\sim 2.6 \times 10^{-8} n^{1/3}$ eV for relaxed material indeed takes an intermediate place between values construed by experiments related to the luminescence peak alone, on the one hand,[6] or to the low energy BE luminescence slope, on the other hand.[7] The value for relaxed material corresponds to what one would expected according to Casey and Stern.[19]

The experimental BE peak full widths at half maximum (FWHM) are plotted as a function of n in Fig. 2(b). The FWHM is compared with the root-mean-squares sum of two broadening components $\Delta = (\Delta_i^2 + E_f^2)^{1/2}$, where the first ($\Delta_i$) is the intrinsic thermal broadening of the NID sample and the second (E_f) is the calculated Fermi energy. The potential fluctuations in the band tail reaching $V_{rms} \sim 35$ meV at $n \sim 10^{19}$ cm^{-3} explain why the determination of the BGN using the low energy PL slope alone, overestimates narrowing.[7] This curve further exhibits the importance of band filling in explaining the broadening.[8]

The external absolute BE photon yield is plotted as a function of n in Fig. 3. Values are normalized according to the number of photons obtained per 1 keV of injected electron energy. The intensity of the BE emission is known to increase as the doping level increases.[8] We observe direct proportionality between the absolute external BE photon yield and n, over two decades in the free electron concentra-
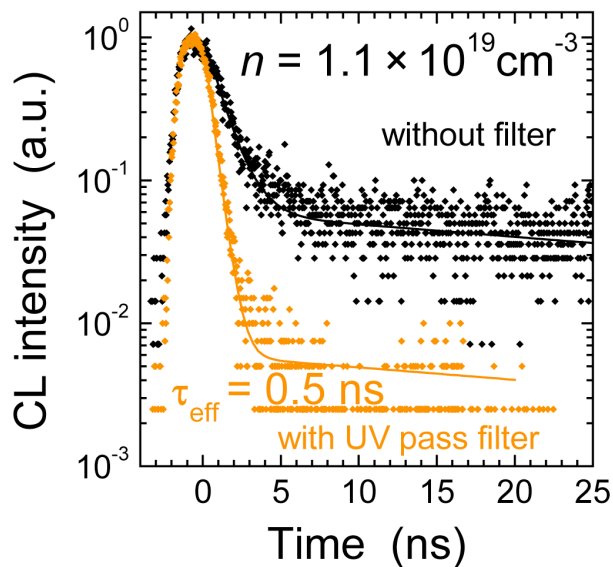
FIG. 4. (Color online) Typical CL decay transients of *n*-type GaN measured with and without UV pass filter. The sample contained a free electron concentration of 1.1×10^{19} cm^{-3} and was maintained at room temperature.

tion. The increase in the external photon yield can consistently be explained by the increase in the internal radiative efficiency $\eta_i = R_{sp} \tau_{eff}$ deduced from Eq. (1). As shown above, $R_{sp} = Bn$, thus

$$\eta_i = Bn \ \tau_{eff}. \quad (6)$$

The external photon yield Y is related to the internal radiation efficiency, η_i by $Y = (1000 \text{ eV}/E_g)\xi\eta_i$, where ξ is the two facet extraction coefficient, given by $\xi = 1 - (1 - n_{ref}^{-2})^{1/2}$, and where n_{ref} is the refractive index. Using $n_{ref} = 2.7$,[20] the relationship between the measured external photon yield and the internal radiative efficiency is $(Y/\eta_i) \sim 21$. Using this argument, the right vertical axis of Fig. 3 is drawn for η_i. Accordingly, 1.4 ± 0.2 photons per 1 keV incident electron obtained on the sample with $n = 1.1 \times 10^{19}$ cm^{-3}, correspond to $\eta_i = 0.07 \pm 0.01$. This value is consistent with the factor of 5.8 ± 0.5 increase in the integrated BE CL intensity that has invariably been observed upon cool down from RT to 77 K, from which (assuming nonradiative recombination centers being thermally activated)[15] an upper limit to the RT internal radiative efficiency of $\eta_i < 0.16 - 0.19$ could be deduced.

RT CL decay of one NID ($n \sim$ mid-10^{17} cm^{-3}) and four Si-doped samples ($n = 1 \pm 0.5 \times 10^{18} - 1.1 \times 10^{19}$ cm^{-3}) was measured, as shown in Fig. 4. Unfiltered CL decay shows contributions from at least two components. When a UV pass filter is used, the second YB component is suppressed. The initial, BE-related fast component, τ_{eff} then dominates the CL intensity decay between one (low n) and over two orders of magnitude (high n). By fitting the CL decay transients, $I(t)$, using $I(t) = I_0 \exp(-t/\tau_{eff})$, the effective BE decay time τ_{eff} is determined. The experimental values scatter between 0.9 and 0.4 ns within the ensemble of the investigated samples. Using the value of $\tau_{eff} = 0.5 \pm 0.1$ ns that is obtained for the most efficient sample ($n = 1.1 \times 10^{19}$ cm^{-3} and $\eta_i = 0.07 \pm 0.01$) we obtain $B = (1.2 \pm 0.3) \times 10^{-11}$ cm^3 s^{-1}.

Based on Eq. (6), we have plotted a line in Fig. 3, as well as two additional lines comprising the scatter of τ_{eff}. The agreement between the values of η_i, n, and τ_{eff} for our samples is markedly good. The extracted value for B is further in good agreement with Ref. 15. Using $\eta_i = \tau_{eff}/\tau_R$ and $1/\tau_{eff} = 1/\tau_R + 1/\tau_{NR}$, linking the radiative (τ_R) with the nonradiative and the effective lifetime, we estimate $\tau_R \gtrsim (15 \pm 2)\tau_{NR}$ for all, including the most efficient sample. The observed effective decay time thus represents, in first approximation, the nonradiative lifetime. The increase in the radiative efficiency with n can consistently be explained by decreasing radiative lifetime with respect to τ_{NR}.[21]

IV. CONCLUSIONS

In conclusion, shift and broadening of the GaN BE luminescence is a result of BGR, of random distribution of the dopants forming states below the gap, and of the upward move of the Fermi energy as n increases. Using the Kane model, we extract the band gap energy and obtain $-(3.58 \pm 0.6) \times 10^{-8}$ and $-(2.56 \pm 0.6) \times 10^{-8} n^{1/3}$ eV for its narrowing in epitaxially strained and in relaxed GaN:Si, respectively. Internal radiative efficiency η_i is found proportional to n over two orders of magnitude reaching $\eta_i = 0.07 \pm 0.01$ at $n = 1.1 \times 10^{19}$ cm^{-3}, which corresponds to an increasing radiative recombination rate according to $B = (1.2 \pm 0.3) \times 10^{-11}$ cm^3 s^{-1}.

[1] H. C. Casey, Jr. and M. B. Panish, *Heterostructure Lasers Part A* (Academic, Orlando, 1978), pp. 131–143.
[2] S. C. Jain, J. M. McGregor, and D. J. Roulson, J. Appl. Phys. **68**, 3747 (1990).
[3] C. Persson, B. E. Sernelius, A. Ferreira da Silva, C. Moysés Araújo, R. Ahuja, and B. Johansson, J. Appl. Phys. **92**, 3207 (2002).
[4] R. Czernetzki, M. Leszczyński, I. Grzegory, P. Perlin, P. Prystawko, C. Skierbiszewski, M. Krysko, M. Sarzyński, P. Wiśniewski, G. Nowak, A. Libura, S. Grzanka, T. Suski, L. Dmowski, E. Litwin-Staszewska, M. Boćkowski, and S. Porowski, Phys. Status Solidi A **200**, 9 (2003).
[5] T. S. Moss, Proc. Phys. Soc. London, Sect. B **67**, 775 (1954); E. Burstein, Phys. Rev. **93**, 632 (1954).
[6] I.-H. Lee, J. J. Lee, P. Kung, F. J. Sanchez, and M. Razeghi, Appl. Phys. Lett. **74**, 102 (1999); H. C. Yang, T. Y. Lin, M. Y. Huang, and Y. F. Chen, J. Appl. Phys. **86**, 6124 (1999).
[7] M. Yoshikawa, M. Kunzer, J. Wagner, H. Obloh, P. Schlotter, R. Schmidt, N. Herres, and U. Kaufmann J. Appl. Phys. **86**, 4400 (1999); Fitting of the RT line broadening is performed using a Fermi energy expression, suitable for zero degree Kelvin only. See, for example, J. De-Sheng, Y. Makita, K. Ploog, and H. J. Queisser, *ibid.* **53**, 999 (1982); M. Leroux, B. Beaumont, N. Grandjean, P. Lorenzini, S. Haffouz, P. Vennéguès, J. Massies, and P. Gibart, Mater. Sci. Eng., B **50**, 97 (1997).
[8] E. F. Schubert, I. D. Goepfert, W. Grieshaber, and J. M. Redwing, Appl. Phys. Lett. **71**, 921 (1997). We find, as shown in Fig. 2(b), that the move of the Fermi energy into the conduction band must *not* be ignored.
[9] G. Borghs, K. Bhattacharyya, K. Deneffe, P. Van Mieghem, and R. Mertens, J. Appl. Phys. **66**, 4381 (1989).

[10] E. Frayssinet, B. Beaumont, J. P. Faurie, P. Gibart, Zs. Makkai, B. Pécz, P. Lefebvre, and P. Valvin, MRS Internet J. Nitride Semicond. Res. **7**, 8 (2002).

[11] S. O. Kucheyev, M. Toth, M. R. Phillips, J. S. Williams, and C. Jagadish, Appl. Phys. Lett. **79**, 2154 (2001).

[12] S. Khatsevich, D. H. Rich, S. Keller, and S. P. DenBaars, Phys. Rev. B **75**, 035324 (2007).

[13] For a review of the above expression, see, e.g., B. G. Yacobi and D. B. Holt, *Cathodoluminescence Microscopy of Inorganic Solids* (Plenum, New York, 1990); The average carrier generation rate per unit volume is given by $G_r \sim I_b V_b / (3 E_g V_{ex})$ where I_b is the beam current, V_b is the acceleration voltage, E_g is the band gap of GaN, and V_{ex} is the estimated *e-h* excitation volume which depends on V_b.

[14] See, for example, W. Liu, M. F. Li, S. J. Xu, K. Uchida, and K. Matsumoto, Semicond. Sci. Technol. **13**, 769 (1998); D. G. Chtchekine, G. D. Gilliland, Z. C. Feng, S. J. Chua, D. J. Wolford, S. E. Ralph, M. J. Schurman, and I. Ferguson, MRS Internet J. Nitride Semicond. Res. **4S1**, G6.47

[15] J. S. Im, A. Moritz, F. Steuber, V. Härle, F. Scholz, and A. Hangleiter, Appl. Phys. Lett. **70**, 631 (1997).

[16] I. Vurgaftman and J. R. Meyer, J. Appl. Phys. **94**, 3675 (2003).

[17] M. Leroux, H. Lahrèche, F. Semond, M. Laügt, E. Feltin, N. Schnell, B. Beaumont, P. Gibart, and J. Massies, Mater. Sci. Forum **353–356**, 795 (2001); H. Lahrèche, M. Leroux, M. Laügt, M. Vaille, B. Beaumont, and P. Gibart, J. Appl. Phys. **87**, 577 (2000).

[18] L. T. Romano, C. G. Van de Walle, J. W. Ager III, W. Götz, and R. S. Kern, J. Appl. Phys. **87**, 7745 (2000).

[19] H. C. Casey, Jr. and F. Stern, J. Appl. Phys. **47**, 631 (1976).

[20] D. Brunner, H. Angerer, E. Bustarret, F. Freudenberg, R. Höpler, R. Dimitrov, O. Ambacher, and M. Stutzmann, J. Appl. Phys. **82**, 5090 (1997).

[21] H. B. Bebb and E. W. Williams, in *Semiconductors and Semimetals*, edited by R. K. Willardson and A. C. Beers (Academic, New York, 1972), Vol. 8, p. 213.